

Estimating the distribution of dynamic invariants: illustrated with an application to human photo-plethysmographic time series

Michael Small

*Department of Electronic and Information Engineering
Hong Kong Polytechnic University, Hung Hom, Kowloon, Hong Kong*

(Dated: November 15, 2018)

Dynamic invariants are often estimated from experimental time series with the aim of differentiating between different physical states in the underlying system. The most popular schemes for estimating dynamic invariants are capable of estimating confidence intervals, however such confidence intervals do not reflect variability in the underlying dynamics. In this communication we propose a surrogate based method to estimate the expected distribution of values under the null hypothesis that the underlying deterministic dynamics are stationary. We demonstrate the application of this method by considering four recordings of human pulse waveforms in differing physiological states and provide conclusive evidence that correlation dimension is capable of differentiating between three (but not all four) of these states.

PACS numbers: 05.45.-a, 05.45.Tp, 05.10.-a

Various dynamic invariants are often estimated from time series in a wide variety of scientific disciplines. It has long been known that these estimates (and in particular correlation dimension estimates) alone are not sufficient to differentiate between chaos and noise. Most notably, the method of surrogate data [1] was introduced in an attempt to reduce the rate of false positives during the hunt for physical examples of chaotic dynamics. Although it is not possible to find conclusive evidence of chaos through estimation of dynamic invariants, surrogate methods are used to generate a distribution of statistic (i.e. the estimates of the dynamic invariant) values under the hypothesis of linear noise. In the most general form, the standard surrogate methods can generate the distribution of statistic values under the null hypothesis of a static monotonic nonlinear transformation of linearly filtered noise.

In this communication, we introduce a significant generalisation of a recent surrogate generation algorithm [2, 3]. The *pseudo-periodic surrogate* (PPS) algorithm allows one to generate data consistent with the null hypothesis of a noise driven periodic orbit — provided the data exhibits pseudo-periodic dynamics. This algorithm has been applied to differentiate between a noisy limit cycle, and deterministic chaos. By modifying this algorithm and applying it to noisy time series data, we are able to generate surrogate time series that are independent trajectories of the same deterministic system.

This ensemble of *attractor trajectory surrogates* (ATS) can then be used to estimate the distribution statistic values for estimates of any statistic derived from these time series. The statistics of greatest interest to us are dynamic invariants of the underlying attractor, and in particular correlation dimension and entropy estimates provided by the *Gaussian kernel algorithm* (GKA) [4, 5]. Our choice of the GKA is entirely arbitrary, but based on our familiarity with this particular algorithm.

An important application for the ATS technique is to determine whether dynamic invariants estimated from

distinct time series are significantly different. The question this technique can address is whether (for example) a correlation dimension of 2.3 measured during normal electrocardiogram activity is really distinct from the correlation dimension of 2.4 measured during an episode of ventricular tachycardia [6, 7]. Estimates of dynamic invariants (including the GKA [4, 5]) often come with confidence intervals. But these confidence intervals can only be based on uncertainty in the least-mean-square fit, not the underlying dynamics. Conversely, it is standard practice to obtain a large number of representative time series for each (supposedly distinct) physical state, and compare the distribution of statistic values derived from these. But, this approach is not always feasible: in [6, 7] for example, the problem is not merely that these physiological states are both difficult and dangerous to replicate, but that inter-patient variability makes doing so infeasible.

In the remainder of this communication we describe the new ATS algorithm and demonstrate that it can be used to estimate the distribution of dynamic invariant estimates from a single time series of a known dynamical system (the chaotic Rössler system). We then apply this same method to four recordings of human pulse waveforms, measured via photo-plethysmography [8, 9]. Each of the four recordings correspond to a distinct physiological state. We compute correlation dimension and entropy using the GKA method and show that the expected distribution of correlation dimension and entropy estimates are sufficient to differentiate between these four physiological states.

The ATS algorithm may be described as follows. Embed a scalar time series $\{x_t\}$ to obtain a vector timeseries $\{z_t\}$ (of length N). The choice of embedding is arbitrary, but has been adequately discussed in the literature ([10] for example). From the embedded time series, the surrogate is obtained as follows. Choose an initial condition, $w_1 \in \{z_t | t = 1, \dots, N\}$. Then, at each step, choose the

successor to w_t with probability

$$P(w_{t+1} = z_{i+1}) \propto \exp \frac{-\|w_t - z_i\|}{\rho} \quad (1)$$

where the *noise radius* ρ is an as-yet unspecified constant. In other words, the successor to w_t is the successor of a randomly chosen neighbour of w_t . Finally, from the vector time series $\{w_t\}$ the ATS $\{s_t\}$ is obtained by projecting w_t onto $[1 \ 0 \ 0 \ 0 \ \dots \ 0]$ (the first coordinate). Hence

$$s_t = w_t \cdot [1 \ 0 \ 0 \ 0 \ \dots \ 0] \quad (2)$$

In [2, 3] this algorithm was shown to be capable of differentiating between deterministic chaos and a noisy periodic orbit. In the context of the current communication we assume that $\{x_t\}$ is contaminated by additive (but possibly dynamic) noise and we choose the noise radius ρ such that the observed noise is replaced by an independent realisation of the same noise process. Furthermore, we assume that the deterministic dynamics are preserved by suitable choice of embedding parameters. Under these two assumptions, $\{z_t\}$ and $\{w_t\}$ have the same invariant density and $\{x_t\}$ and $\{s_t\}$ are therefore (noisy) realisation of the same dynamical system with (for suitable choice of ρ) the same noise distribution.

As in [2, 3] the problem remains the correct choice of ρ . This is the major difference between the ATS described here and the PPS of [2, 3]. However, since the null hypothesis we wish to address is different from (and more general than) that of the PPS, choice of ρ for the ATS is less restrictive. For $t = T$ given, one can compute $P(w_{t+1} \neq z_{i+1} \wedge \|w_t - z_i\| = 0 | t = T)$ directly from the data by applying (1). Assuming the process is ergodic [11] one can then sum

$$P(w_{t+1} \neq z_{i+1} \wedge \|w_t - z_i\| = 0) = \frac{1}{N} \sum_{T=1}^N P(w_{t+1} \neq z_{i+1} \wedge \|w_t - z_i\| = 0 | t = T) \quad (3)$$

to get the probability of a temporal discontinuity [12] in the surrogate at any time instant. There is a 1:1 correspondence between a value $p = P(w_{t+1} \neq z_{i+1} \wedge \|w_t - z_i\| = 0)$ and ρ , and we choose to implement (1) for a particular value of p (i.e. a particular transition probability) rather than a specific noise level. In what follows we find that studying intermediate values of p ($p \in [0.05, 0.95]$) is sufficient. However, the significant point is that $p \in [0.05, 0.95]$ corresponds to a very narrow range of values of ρ .

We now demonstrate the applicability of this method for noisy time series data simulated from the Rössler differential equations (during “broad-band” chaos). We integrated (1000 points with a time step of 0.2) the Rössler equations both with and without multidimensional dynamic noise at 5% of the standard deviation of the data. We then studied the x -component after the addition of

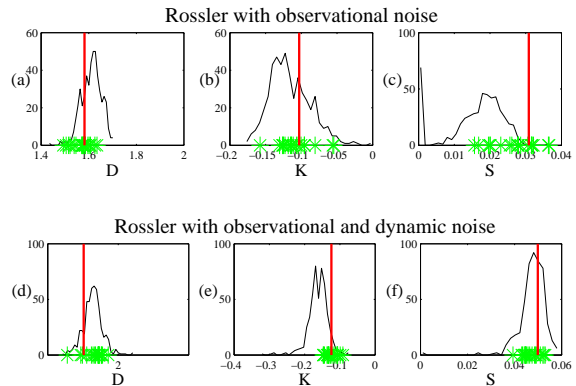


FIG. 1: **Distribution of statistics D , K and S for short and noisy realisations of the Rössler system.** The histogram shows the distribution of statistic estimates (D , K and S) for 500 ATS time series generated from a 1000 point realisation of the Rössler system. The solid vertical line on each plot is the comparable value for the data and the stars marked on the horizontal axes are for 20 independent realisations of the same process. The top row of figures depicts results for the Rössler system with observational noise only, the bottom row of figures has both observational and dynamic noise. Panels (a) and (d) show correlation dimension estimates, (b) and (e) are entropy, and (c) and (f) are noise level.

5% observational noise. We selected embedding parameters using the standard methods ($d_e = 3$ and $\tau = 8$) and then compute ATS surrogates for various exchange probabilities $p = 0.05, 0.1, 0.15, \dots, 0.95$. For the data set and each ensemble of surrogates we then estimated correlation dimension D , entropy K and noise level S using the GKA algorithm [4, 5] (GKA embedding using embedding dimension $m = 2, 3, \dots, 10$ and embedding lag of 1). Figure 1 depicts the results when the GKA is applied with embedding dimension $m = 4$ and the exchange probability is $p = 0.35$. Other values of m gave equivalent results, as did various values of p in the range $[0.2, 0.8]$.

For $p \in [0.2, 0.8]$ we found that the estimate of noise S from the GKA algorithm coincided for data and surrogates, but this was often not the case for extreme values of p . Therefore, this estimate of signal noise content is a good indicator of the accuracy of the dynamics reproduced by the ATS time series. Furthermore to confirm the spread of the data we also estimated D , K , and S for 20 further realisations of the same Rössler system (with different initial conditions). In each case, as expected, the range of these values lies well within the range predicted by the ATS scheme.

We now consider the application of this method to photo-plethysmographic recordings of human pulse dynamics over a short time period (about 16.3 seconds). We have access to only a limited amount of data representative of each of four different dynamic regimes. In any case, we would expect the system dynamics to change

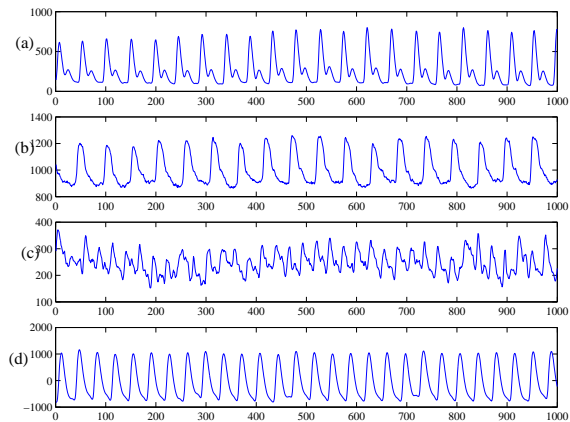


FIG. 2: **Human pulse waveform recorded with photoplethysmography.** Four recordings of human pulse waveform (61 Hz) in four different physiological conditions. The four time series correspond to: (a) normal, (b) quasi-stable, (c) unstable, and (d) post-operative (stable).

if measured over a significantly longer time frame. The data collection and processing with the methods of nonlinear time series analysis are described in [8, 9]. Previously, we have studied nonlinear determinism in cardiac dynamics measured with electrocardiogram (ECG) [6, 7]. Although we do not consider ECG data here, this data would be another useful system to examine with these methods [13]. The four data sets we examine in this communication are depicted in figure 2.

For each data set we repeated the analysis described for the Rössler time series. Results for GKA embedding dimension $m = 4$ and $p = 0.35$ are depicted in figure 3. As with the Rössler system, variation of the parameters m and p did not significantly change the results. We find that in every case (except for $p \notin [0.2, 0.8]$) the distribution of D , K and S estimated from the ATS data using the GKA included the true value. Most significantly, this indicates that the range of values of p is appropriate. Moreover, these results are consistent with the hypotheses that the noise is effectively additive and can be modelled with this simple scheme, and that the underlying deterministic dynamics can be approximated with a local constant modelling scheme.

We also estimated the statistics D , K and S for additional available data (subsequent, contiguous, but non-overlapping) from each of the four rhythms. This small amount of data afforded us two or three additional estimates of each statistic for each rhythm. For the unstable and quasi-stable rhythm we observed good agreement. For the stable (normal and post-operative) rhythms, this is not the case. On examination of the data we find that this result is to be expected. Both the stable rhythms undergo a change in amplitude and baseline subsequent to the end of the original 16 second recording, this non-stationarity is reflected in the results. This same

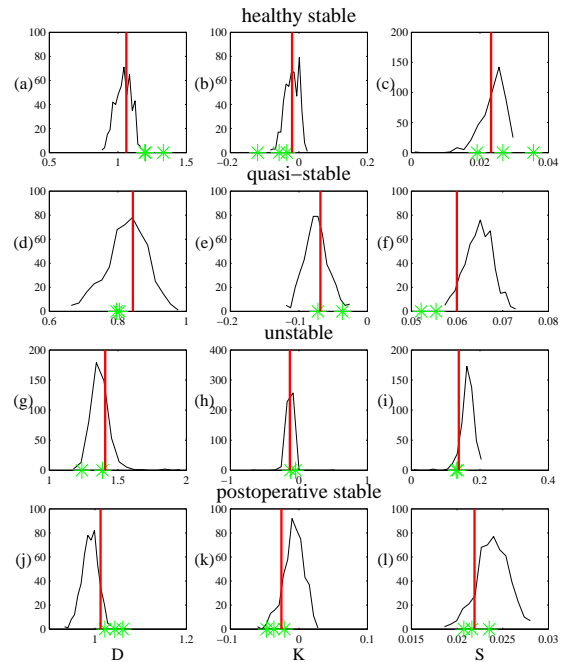


FIG. 3: **Distribution of statistics D , K and S for human pulse waveforms.** The histogram shows the distribution of statistic estimates (D , K and S) for 500 ATS time series generated from each of the four time series depicted in figure 2. The solid vertical line on each plot is the comparable value for the data and the stars marked on the horizontal axes are for the (limited) subsequent data recorded from each patient. In each case only two or three subsequent contiguous but non-overlapping timeseries were available. The figures are: (a) correlation dimension (D), (b) entropy (K), and (c) noise (S) for the normal rhythm; (d) D , (e) K , and (f) S for the quasi-stable rhythm; (g) D , (h) K , and (i) S for the unstable rhythm; and (j) D , (k) K , and (l) S for the post-operative stable rhythm.

non-stationarity has also been observed independently in Bhattacharya and co-workers [8, 9].

We now return to the question that the ATS test was designed to address: can we differentiate between these four rhythms based on the GKA? Figure 4 provides the answer. In figure 4 we see the estimated distribution of statistic values (D , K and S) for each of the four rhythms shown in figure 2. Clearly (and not surprisingly), the correlation dimension estimate and noise level of the unstable rhythm is significantly different from the other three rhythms. More significantly, the quasi-stable rhythm is also observed to be distinct from the other three regimes. Furthermore, we observe that in the quasi-stable state the correlation dimension estimate is significantly less than one, while for the unstable state it is significantly larger than one. For example, the quasi-stable state may be characterised by a noise driven stable focus [14], while the unstable state exhibits high dimensional (i.e. $D > 1$) deterministic dynamics. Both these regimes exhibit sig-

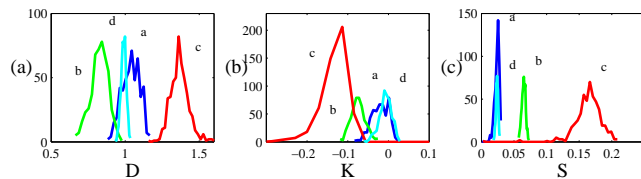


FIG. 4: **Discriminating power of the statistics D , K and S for human pulse waveforms.** The distribution (a binned histogram) of statistic values estimated via the ATS method (as described in figure 3) for each of the four distinct physiological waveforms is shown. The four rhythms are labelled 'a', 'b', 'c', and 'd' corresponding to the same labelling in figure 2. These figures show that correlation dimension alone is sufficient to differentiate between three of these four physiological states. The exception is that these three statistics are insufficient to differentiate between the normal and post-operative states.

nificantly more (additive Gaussian) noise than the stable states.

The two stable states (panels (a) and (d) of figure 2) are harder to distinguish: both visually and using the statistics D , K , and S . While the individual data sets we depict in figure 2 exhibit different statistic values (for example $D = 1.06$ and $D = 1.01$), we find that the ATS analysis indicates that these statistics are not significantly different. Both regimes exhibit a correlation dimension of about one, and a similar noise level. The variation in observed results is lesser in the post-operative stable regime, but the distribution do overlap.

Finally, we find that entropy estimated with the GKA algorithm K is of no use in differentiating between these four rhythms.

The results of this analysis are in general agreement with those presented in [8, 9]. Independent linear surrogate analysis [1] has confirmed that each of these

four rhythms is inconsistent with a monotonic nonlinear transformation of linearly filtered noise [15]. The only significant difference is that the correlation dimension estimates we present here are significantly lower than those in [8, 9]. This is due to the different correlation dimension algorithm. Unlike the algorithm employed in [8, 9], the GKA separates the data into purely deterministic and stochastic components, and hence estimates both D and S . The correlation dimension estimated in [8, 9] is the combined effect of both components of the GKA.

Although we have considered the specific application of human pulse dynamics, the algorithm we have proposed may be applied to a wide variety of problems. We have shown that provided time delay embedding parameters can be estimated adequately, and an appropriate value of the exchange probability is chosen, the ATS algorithm generates independent trajectories from the same dynamical system. When applied to data from the Rössler system we confirm this result, and we demonstrate its application to experimental data.

When the ATS algorithm is applied to generate independent realisation for a hypothesis test, one is able to construct a test for non-stationarity. If two data sets do not fit the same distribution of ATS data then they can not be said to be from the same deterministic dynamical system. Unfortunately, the converse is not always true and the power of the test depends on the choice of statistic. The utility of this technique as a test for stationarity remains a subject for future investigation.

Acknowledgments

This research was supported by a Hong Kong Polytechnic University Research Grant (NO. A-PE46). The authors wish to thank J. Bhattacharya for supplying the photo-plethysmographic time series.

-
- [1] J. Theiler *et al.* *Physica D*, 58:77–94, 1992.
 - [2] M. Small, D. Yu, and R.G. Harrison. *Physical Review Letters*, 87:188101, 2001.
 - [3] M. Small and C.K. Tse. *Physica D*, 164:187–201, 2002.
 - [4] C. Diks. *Physical Review E*, 53:R4263–R4266, 1996.
 - [5] D. Yu *et al.* *Physical Review E*, 61:3750–3756, 2000.
 - [6] M. Small *et al.* *Chaos, Solitons and Fractals*, 13:1755–1762, 2001.
 - [7] M. Small *et al.* *Computers in Cardiology*, 27:355–358, 2000.
 - [8] J. Bhattacharya and P.P. Kanjilal. *IEEE Transactions on Systems, Man and Cybernetics A*, 29:406–410, 1999.
 - [9] J. Bhattacharya, P.P. Kanjilal, and V. Muralidhar. *IEEE Transactions on Biomedical Engineering*, 48:5–11, 2001.
 - [10] M. Small and C.K. Tse. *Physica D*, 2003. To appear.
 - [11] This assumption is sufficient rather than necessary.
 - [12] By temporal discontinuity we mean that $w_t = z_i$ but $w_{t+1} \neq z_{i+1}$.
 - [13] Actually, the problem here is that we have too much data and it is therefore difficult to select a “representative” small number of short time series. However, we intend to examine this data more carefully in forthcoming work.
 - [14] Due to the discretisation necessary to digitise this data, a noise drive stable periodic orbit is also a plausible cause of the observed data. To distinguish these two, a more detailed study is required.
 - [15] These calculations are routine, and not presented in this communication.